

# A Theoretical Study of the C–H Activation of Methane Derivatives. Significant Effects of Electron-Withdrawing Substituents

Shigeyoshi Sakaki,\* Bishajit Biswas, and Manabu Sugimoto

Department of Applied Chemistry and Biochemistry, Faculty of Engineering, Kumamoto University, Kurokami, Kumamoto 860, Japan

Received August 11, 1997

The  $sp^3$  C–H activation of  $CH_3CN$  and  $CH_2(CN)_2$  by palladium(0) complexes was theoretically investigated with the ab initio MO/MP4 method. Although introduction of an electron-withdrawing CN group lowers the activation energy ( $E_a$ ) and decreases the endothermicity ( $E_{endo}$ ),  $E_a$  and  $E_{endo}$  are still high in C–H activation by a palladium(0) monodentate phosphine model complex,  $Pd(PH_3)_2$ :  $E_a = 37$  kcal/mol and  $E_{endo} = 34$  kcal/mol for  $CH_4$ ,  $E_a = 32$  kcal/mol and  $E_{endo} = 23$  kcal/mol for  $CH_3CN$ , and  $E_a = 25$  kcal/mol and  $E_{endo} = 11$  kcal/mol for  $CH_2(CN)_2$ , where MP4SDQ values are given. However,  $E_a$  becomes significantly low and the reaction becomes exothermic in the C–H activation of  $CH_2(CN)_2$  by a chelate phosphine model complex;  $E_a = 18$  kcal/mol and  $E_{exo} = 11$  kcal/mol in a simple model Pd(dipe) in which two  $PH_3$  ligands are placed to mimic bis(dicyclohexylphosphino)ethane, and  $E_a = 19$  kcal/mol and  $E_{exo} = 6$  kcal/mol in a more realistic model  $Pd(H_2PCH_2-CH_2PH_2)$ . The acceleration by the CN group is interpreted in terms of the charge-transfer interaction from Pd to the  $\pi^*$  orbital of  $CH_2(CN)_2$  into which the C–H  $\sigma^*$  orbital mixes. These computational results suggest that the C–H activation by a palladium(0) complex easily occurs when electron-withdrawing groups are introduced on the  $sp^3$  carbon atom and a chelate phosphine is used as a ligand.

## Introduction

The  $sp^3$  C–H activation of alkane is one of challenging research subjects in organometallic chemistry, since the  $sp^3$  C–H activation would lead to new catalytic reactions for utilization of hydrocarbon compounds.<sup>1</sup> However,  $sp^3$  C–H activation is difficult, because the  $sp^3$  C–H  $\sigma^*$  orbital is at a high energy and its  $\sigma$  orbital is at a low energy. Thus, many experimental efforts have been made to perform  $sp^3$  C–H activation by using highly reactive and coordinatively unsaturated transition metal complexes.<sup>1–8</sup> Not only experimental works but also many theoretical works have been carried out on the C–H activation by transition metal complexes, to present detailed understanding of the  $sp^3$  C–H

activation.<sup>9–13</sup> In those studies, we cannot find results that  $sp^3$  C–H activation was successfully carried out with a palladium(0) complex. In fact, an ab initio MO theoretical study clearly demonstrated that the C–H activation by a palladium(0) complex is much difficult and the reverse C–H coupling reaction easily occurs with no barrier.<sup>11a</sup> This is not surprising because the palladium d orbital is at a low energy.

However, Yamamoto and his collaborators recently succeeded in the palladium-catalyzed addition of activated methylene and methyne to allene and they proposed the reaction mechanism in which the palladium(0) complex performs  $sp^3$  C–H activation of methane derivatives including such electron-withdrawing groups as CN and  $CO_2Et$ .<sup>14</sup> Also, similar  $sp^3$  C–H

(1) For instance see: (a) Shilov, A. E. *Activation of Saturated Hydrocarbons by Transition Metal Complexes*; D. Reidel: Boston, MA, 1984. (b) Crabtree, R. H. *Chem. Rev.* **1985**, *85*, 245. (c) Ryabov, A. D. *Chem. Rev.* **1990**, *90*, 403. (d) Bergman, R. G. *J. Organomet. Chem.* **1990**, *400*, 273. (e) Arndtsen, B. A.; Bergman, R. G.; Mobley, T. A.; Peterson, T. H. *Acc. Chem. Res.* **1995**, *28*, 154.

(2) Gianotti, C.; Green, M. L. H. *J. Chem. Soc., Chem. Commun.* **1972**, 1114.

(3) (a) Crabtree, R. H.; Miheleic, J. M.; Quirk, J. M. *J. Am. Chem. Soc.* **1979**, *101*, 7738.

(4) Jones, W. D.; Feher, F. J. *J. Am. Chem. Soc.* **1982**, *104*, 4240; *Organometallics* **1983**, *2*, 562

(5) (a) Hoyano, J. K.; Graham, W. A. *J. Am. Chem. Soc.* **1982**, *104*, 3723. (b) Hoyano, J. K.; McMaster, A. D.; Graham, W. A. *J. Am. Chem. Soc.* **1983**, *105*, 7190.

(6) (a) Janowicz, A. H.; Bergman, R. G. *J. Am. Chem. Soc.* **1982**, *104*, 352; **1983**, *105*, 3929. (b) Wax, M. J.; Kovac, C. A.; Bergman, R. G. *J. Am. Chem. Soc.* **1984**, *106*, 1121.

(7) Hackett, M.; Whitesides, G. M. *J. Am. Chem. Soc.* **1988**, *110*, 1449.

(8) Sakakura, T.; Sodeyama, T.; Sasaki, K.; Wada, K.; Tanaka, M. *J. Am. Chem. Soc.* **1990**, *112*, 7221.

(9) Saillard, J.-Y.; Hoffmann, R. *J. Am. Chem. Soc.* **1984**, *106*, 2006.

(10) (a) Obara, S.; Kitaura, K.; Morokuma, K. *J. Am. Chem. Soc.* **1984**, *106*, 7482. (b) Koga, N.; Morokuma, K. *J. Phys. Chem.* **1990**, *94*, 5454. (c) Koga, N.; Morokuma, K. *J. Am. Chem. Soc.* **1993**, *115*, 6883.

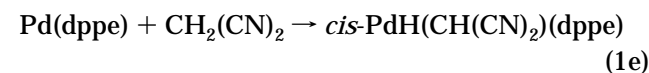
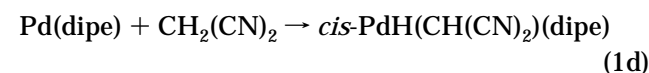
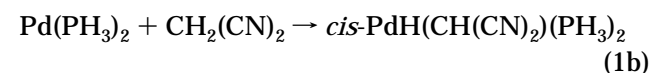
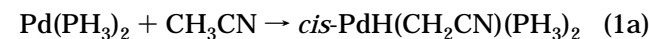
(11) (a) Low, J. J.; Goddard, W. A. *J. Am. Chem. Soc.* **1986**, *108*, 6115. (b) Low, J. J.; Goddard, W. A. *Organometallics*, **1986**, *5*, 609.

(12) (a) Blomberg, M. R. A.; Siegbahn, P. E. M.; Nagashima, U.; Wennerberg, J. *J. Am. Chem. Soc.* **1991**, *113*, 424. (b) Svensson, M.; Blomberg, M. R. A.; Siegbahn, P. E. M. *J. Am. Chem. Soc.* **1991**, *113*, 7076. (c) Blomberg, M. R. A.; Siegbahn, P. E. M.; Svensson, M. *J. Am. Chem. Soc.* **1992**, *114*, 6095. (d) Siegbahn, P. E. M.; Blomberg, M. R. A.; Svensson, M. *J. Am. Chem. Soc.* **1993**, *115*, 4191. (e) Blomberg, M. R. A.; Siegbahn, P. E. M.; Svensson, M. *J. Phys. Chem.* **1994**, *98*, 2062. (f) Siegbahn, P. E. M.; Blomberg, M. R. A. *Organometallics* **1994**, *13*, 354. (g) Siegbahn, P. E. M. *Organometallics* **1994**, *13*, 2833. (h) Siegbahn, P. E. M.; Svensson, M. *J. Am. Chem. Soc.* **1994**, *116*, 10124. (i) Siegbahn, P. E. M. *J. Am. Chem. Soc.* **1996**, *118*, 1487.

(13) (a) Sakaki, S.; Ieki, M. *J. Am. Chem. Soc.* **1993**, *115*, 2373. (b) Sakaki, S.; Biswas, B.; Sugimoto, M. *J. Chem. Soc., Dalton Trans.* **1997**, 803.

activation of CH<sub>3</sub>CN by a ruthenium complex was successfully carried out and applied to the ruthenium-catalyzed Michael reaction by Murahashi and his collaborators.<sup>15</sup> Despite these interesting catalytic reactions, the effects of an electron-withdrawing group on sp<sup>3</sup> C–H activation have not been theoretically investigated in detail, to our knowledge.

In this work, we carried out an ab initio MO study of the C–H activation of CH<sub>3</sub>CN and CH<sub>2</sub>(CN)<sub>2</sub> by palladium(0) complexes (eq 1). Because a chelate phosphine was used as a ligand in the palladium-catalyzed reaction by Yamamoto et al.,<sup>14</sup> we investigated here C–H activation by a monodentate phosphine model complex Pd(PH<sub>3</sub>)<sub>2</sub>, a chelate phosphine model complex Pd(dipe) in which two PH<sub>3</sub> ligands are placed to mimic bis(dicyclohexylphosphino)ethane (see Computational Details for dipe), and a more realistic model of a chelate phosphine complex Pd(dppe) (dppe = H<sub>2</sub>PCH<sub>2</sub>CH<sub>2</sub>PH<sub>2</sub>).



The C–H activation of CH<sub>4</sub> by Pd(dppe) was also investigated here, since this reaction was not yet examined in our previous work.<sup>13b</sup> Our purposes here are to show whether C–H activation of CH<sub>3</sub>CN and CH<sub>2</sub>(CN)<sub>2</sub> can be performed with a palladium(0) complex and to clarify the reason the electron-withdrawing group facilitates the C–H activation of methane derivatives and stabilizes the Pd–alkyl bond. Our intention with this work is to theoretically predict the conditions under which sp<sup>3</sup> C–H activation by a palladium(0) complex easily occurs.

### Computational Details

Geometries of reactants, transition states, and products were optimized at the MP2 level, where the geometry of PH<sub>3</sub> was taken from the experimental structure of the free PH<sub>3</sub> molecule.<sup>16</sup> The transition state was determined by calculating the Hessian matrix. The MP4SDQ calculations were carried out with the MP2-optimized geometries. In all these calculations, the core orbitals were excluded from the active space.

Two kinds of basis set systems, BS-I and BS-II, were employed in this work; BS-I was used for geometry optimization, and BS-II was employed for MP2–MP4SDQ calculations. In BS-I, core electrons of Pd (up to 3d) and P (up to 2p) were replaced with the effective core potentials (ECPs),<sup>17,18</sup> and (311/

311/31) and (21/21/1) basis sets were used for valence electrons of Pd and P,<sup>17,18</sup> respectively, where a d polarization function ( $\zeta = 0.34$ ) was added on P. MIDI-3<sup>19</sup> and (31) sets<sup>20</sup> were used for C, N, and H atoms, respectively. The d ( $\zeta = 0.60$ ) and p ( $\zeta = 1.0$ ) polarization functions were added to the alkyl C and active H atoms, respectively, where the active H atom is the hydride ligand and the H atom of methane derivatives that turns into the hydride ligand in C–H activation. In BS-II, a more flexible (311/311/211) set was used for the valence electrons of Pd,<sup>17</sup> where the ECPs were taken to be the same as those employed in BS-I.<sup>17</sup> The (721/41/1) basis set<sup>20</sup> was used for all C and N atoms. A (31/1) set<sup>20</sup> was employed for the H atom except H of PH<sub>3</sub> and dppe in which the p-polarization function was excluded. The basis set and ECPs adopted for P were taken to be the same as those in BS-I. A p-diffuse function and an f-polarization function were not added to C and Pd, respectively, since they little change the activation energy and the reaction energy in the C–H activation of CH<sub>4</sub> by Pd(PH<sub>3</sub>)<sub>2</sub>.<sup>13b</sup> Gaussian 92<sup>21a</sup> and 94<sup>21b</sup> programs were used for these calculations.

Bis(dicyclohexylphosphino)ethane (dcpe) was selected here as a representative of chelate phosphines, because the X-ray structure of the Pd–dcpe complex was reported.<sup>22</sup> Since dcpe is too large for ab initio MO calculation, this was modeled by placing two PH<sub>3</sub> ligands at the P positions of cis-Pd(SiR<sub>3</sub>)<sub>2</sub>–(dcpe),<sup>22</sup> as follows: the P–P distance was taken to be the same as that of cis-Pd(SiR<sub>3</sub>)<sub>2</sub>(dcpe) and the Pd–X and P(1)–X distances were optimized, where X was a point between P(1) and P(2) and the Pd–X line was taken to be perpendicular to the P(1)–P(2) line (see Scheme 1 of ref 13b). This means that Pd–P(1) and Pd–P(2) distances were optimized under a constraint that the P(1)–P(2) distance was fixed. This model complex is called Pd(dipe) here. Since dipe was a simple model, diphosphinoethane (H<sub>2</sub>PCH<sub>2</sub>CH<sub>2</sub>PH<sub>2</sub>) was also adopted as a more realistic model of dcpe. This is abbreviated here as dppe. Pd(PH<sub>3</sub>)<sub>2</sub> represents a palladium monodentate phosphine model complex.

### Results and Discussion

**Geometry Changes in the C–H Activation of CH<sub>3</sub>CN and CH<sub>2</sub>(CN)<sub>2</sub> by a Monodentate Phosphine Model, Pd(PH<sub>3</sub>)<sub>2</sub>.** Important geometry changes are shown in Figures 1 and 2, in which several unimportant precursor complexes are omitted for brevity. Precursor complexes are grouped into two kinds; one (**PCM1a** and **PCM2a**) involves the η<sup>1</sup>-end-on coordination of the CN group, and the other (**PCM1b** and **PCM2b**) involves the η<sup>2</sup>-side-on coordination of the CN group. Although the η<sup>1</sup>-end-on coordination structure

(18) Wadt, W. R.; Hay, P. J. *J. Chem. Phys.* **1985**, *82*, 284.

(19) Huzinaga, S.; Andzelm, J.; Klobukowski, M.; Radizo-Andzelm, E.; Sakai, Y.; Tatewaki, H. *Gaussian basis sets for Molecular Calculations*; Elsevier: Amsterdam, 1984.

(20) Dunning, T. H.; Hay, P. J. In *Methods of Electronic Structure Theory*; Schaeffer, H. F., Ed.; Plenum: New York, 1977; Vol. 4, p 1.

(21) (a) Frisch, M. J.; Trucks, G. W.; Head-Gordon, M.; Gill, P. M. W.; Wong, M. W.; Foresman, J. B.; Johnson, B. G.; Schlegel, H. B.; Robb, M. A.; Replogle, E. S.; Gomperts, R.; Andres, J. L.; Raghavachari, K.; Binkley, J. S.; Gonzalez, C.; Martin, R. L.; Fox, D. J.; DeFrees, D. J.; Baker, J.; Stewart, J. J. P.; Pople, J. A. *Gaussian 92*; Gaussian Inc., Pittsburgh, PA, 1992. (b) Frisch, M. J.; Trucks, G. W.; Schlegel, H. B.; Gill, P. M. W.; Johnson, B. G.; Robb, M. A.; Cheeseman, J. R.; Keith, T. A.; Petersson, G. A.; Montgomery, J. A.; Raghavachari, K.; Al-Laham, M. A.; Zakrzewski, V. G.; Ortiz, J. V.; Foresman, J. B.; Cioslowski, J.; Stefanov, B. B.; Nanayakkara, A.; Challacombe, M.; Peng, C. Y.; Ayala, P. Y.; Chen, W.; Wong, M. W.; Andres, J. L.; Replogle, E. S.; Gomperts, R.; Martin, R. L.; Fox, D. J.; Binkley, J. S.; DeFrees, D. J.; Baker, J.; Stewart, J. J. P.; Head-Gordon, M.; Gonzalez, C.; Pople, J. A. *Gaussian 94*; Gaussian Inc.: Pittsburgh, PA, 1994.

(22) Pan, Y.; Mague, J. T.; Fink, M. J. *Organometallics* **1992**, *11*, 3495.

(14) Yamamoto, Y.; Al-Masum, M.; Asao, N. *J. Am. Chem. Soc.* **1994**, *116*, 6019.

(15) (a) Murahashi, S.-I.; Hirano, T.; Yano, T. *J. Am. Chem. Soc.* **1978**, *100*, 348. (b) Murahashi, S.-I.; Watanabe, T. *J. Am. Chem. Soc.* **1979**, *101*, 7429. (c) Murahashi, S.-I.; Naota, T.; Taki, H.; Mizuno, M.; Takaya, H.; Komiya, S.; Mizuno, Y.; Oyasato, N.; Hiraoka, M.; Hirano, M.; Fukuoka, A. *J. Am. Chem. Soc.* **1995**, *117*, 12436. (d) Murahashi, S.-I.; Naota, T. *Bull. Chem. Soc. Jpn.* **1996**, *69*, 1805.

(16) Herzberg, G. *Molecular Spectra and Molecular Structure*, Van Nostrand, Princeton, NJ, 1967; Vol. 3, p 610.

(17) Hay, P. J.; Wadt, W. R. *J. Chem. Phys.* **1985**, *82*, 299.

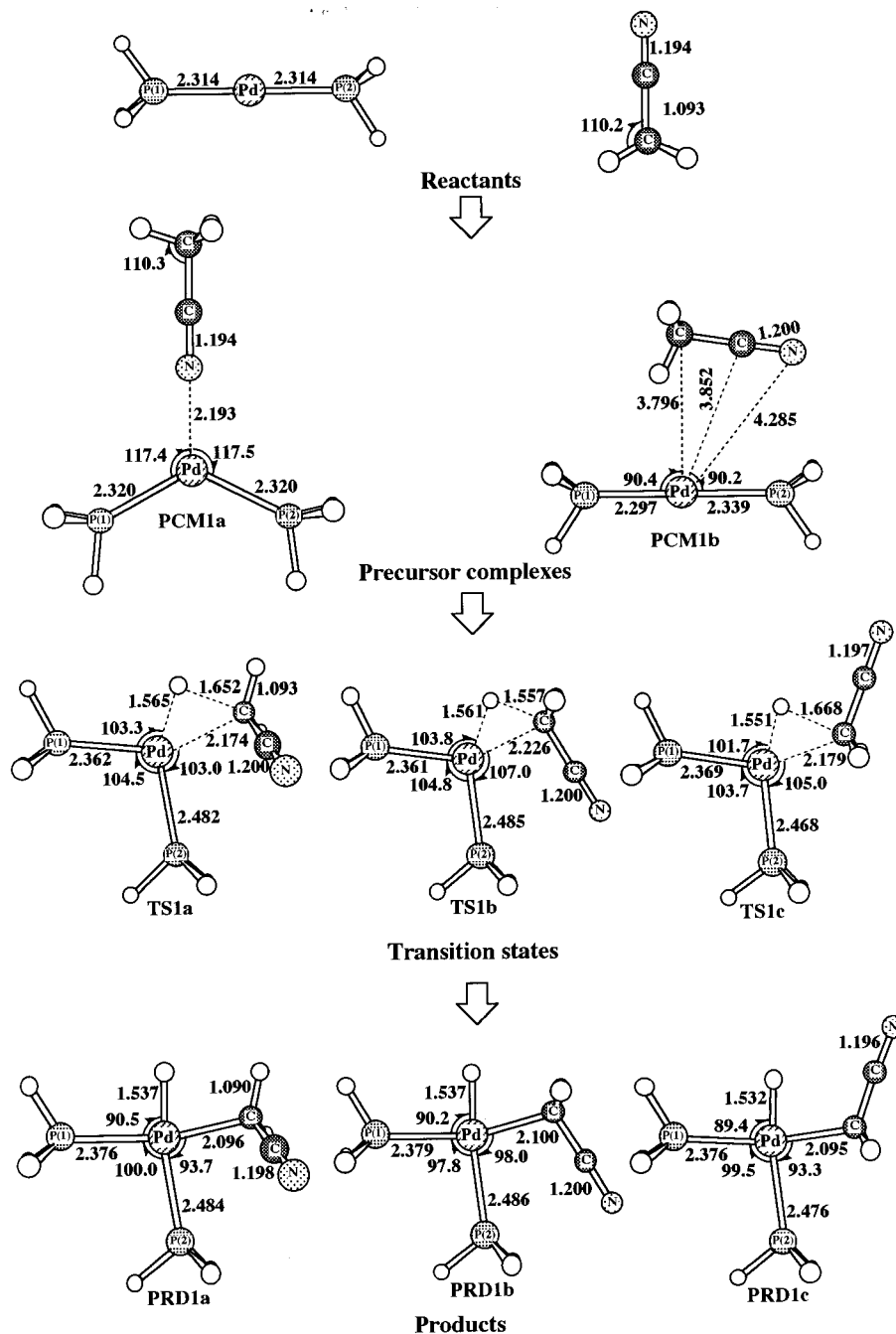


**Figure 1.** Geometry changes in the C-H activation of CH<sub>3</sub>CN by Pd(PH<sub>3</sub>)<sub>2</sub>. Bond lengths are in Å, and bond angles, in deg.

is commonly observed in transition metal acetonitrile complexes, the  $\eta^2$ -side-on coordination structure was recently reported in several low-valent transition metal complexes.<sup>23</sup> Thus, **PCM1b** and **PCM2b** are not surprising because they are zerovalent palladium complexes.

Both Pd(PH<sub>3</sub>)<sub>2</sub> and the methane derivatives (CH<sub>3</sub>CN and CH<sub>2</sub>(CN)<sub>2</sub>) little distort in the precursor complexes except **PCM1a** and **PCM2a** in which CH<sub>3</sub>CN and CH<sub>2</sub>(CN)<sub>2</sub> little distort but the Pd(PH<sub>3</sub>)<sub>2</sub> moiety considerably

distorts. These little distorted geometries of CH<sub>3</sub>CN and CH<sub>2</sub>(CN)<sub>2</sub> clearly indicate that CH<sub>3</sub>CN and CH<sub>2</sub>(CN)<sub>2</sub> do not form a strong interaction with Pd. Although **PCM1a** is the most stable in the precursor complexes of CH<sub>3</sub>CN, this structure does not seem to be on the reaction pathway, since all the C-H bonds are much distant from Pd. In the next stable precursor complex **PCM1b**, one C-H bond takes a position near Pd and this structure seems to lead to the TS shown in Figure 1. Although **PCM1b** is less stable than **PCM1a**, the energy difference between them is only 0.5 kcal/mol (the MP4SDQ energy is given hereafter; the reliability of the MP4SDQ method will be discussed below). Considering this very small energy difference, we can reasonably conclude that **PCM1b** is in the thermal

(23) (a) Anderson, S. J.; Wells, F. J.; Wilkinson, G.; Hussain, B.; Hursthouse, M. B. *Polyhedron* **1988**, *7*, 2615. (b) Chetcuti, P. A.; Knobler, C. B.; Hawthorne, M. F. *Organometallics* **1988**, *7*, 650. (c) Wright, T. C.; Wilkinson, G.; Motevalli, M.; Hursthouse, M. B. *J. Chem. Soc., Dalton Trans.* **1986**, 2017. (d) Barrera, J.; Sabat, M.; Harman, W. D. *J. Am. Chem. Soc.* **1991**, *113*, 8178.

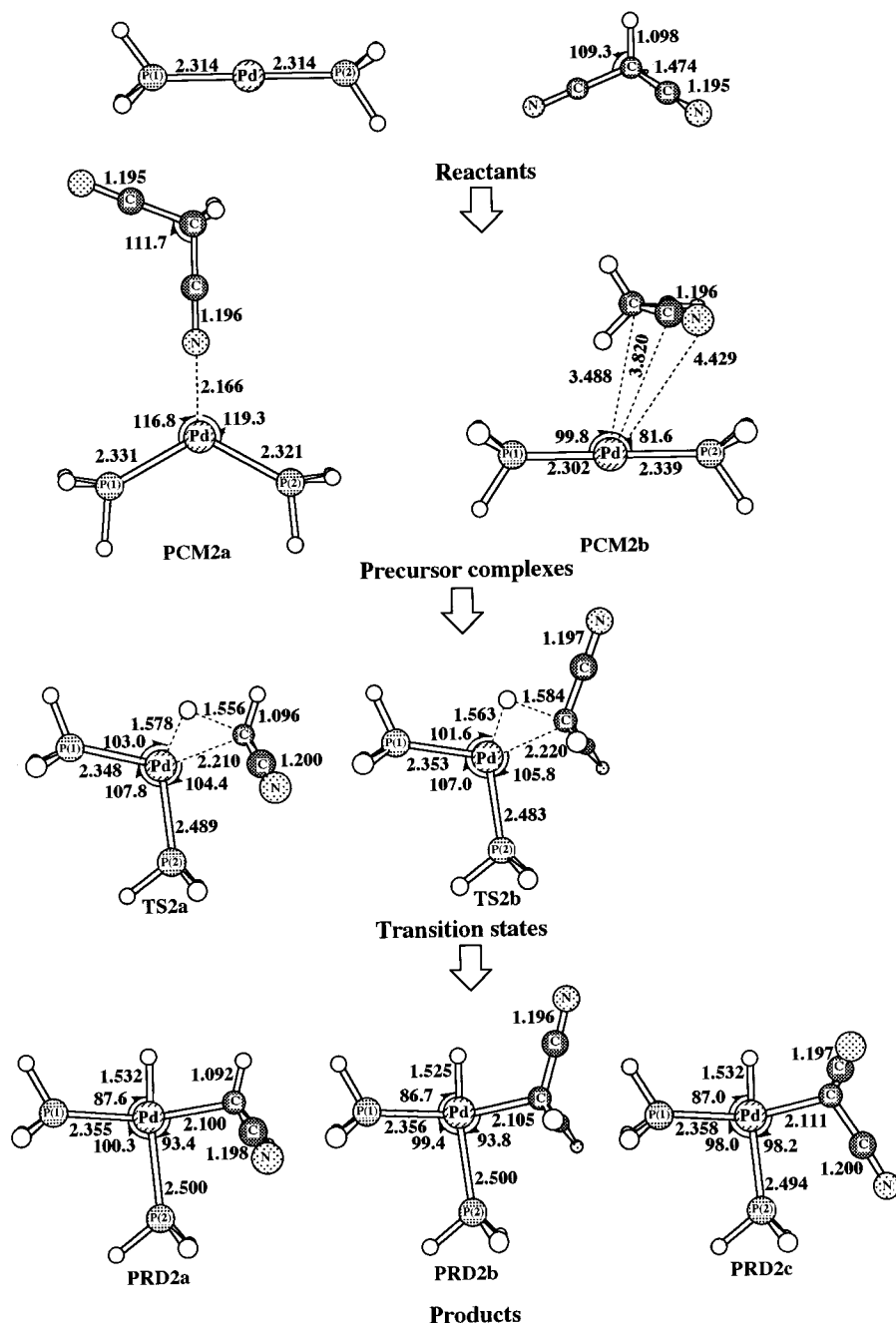


**Figure 2.** Geometry changes in the C–H activation of  $\text{CH}_2(\text{CN})_2$  by  $\text{Pd}(\text{PH}_3)_2$ . Bond lengths are in Å, and bond angles, in deg.

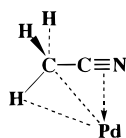
equilibrium with **PCM1a**, and the C–H activation of  $\text{CH}_3\text{CN}$  starts from **PCM1b**. In the precursor complex of  $\text{CH}_2(\text{CN})_2$ , on the other hand, **PCM2b** is the most stable, in which two CN groups interact with Pd in an  $\eta^2$ -side-on coordination structure. **PCM2b** is only 1.3 kcal/mol more stable than **PCM2a** which involves the  $\eta^1$ -end-on coordination structure (Figure 2). Since one C–H bond takes a position near Pd in **PCM2b** like that in **PCM1b**, **PCM2b** is considered to be on the reaction pathway of the C–H activation.

It is important to clarify whether the CN group interacts with Pd in **PCM1b** and **PCM2b**. The CN distance is almost the same as that of free  $\text{CH}_3\text{CN}$ , and the Pd– $\text{CH}_3\text{CN}$  distance is very long. These features suggest that the C≡N group does not form a strong stabilization interaction with Pd, as discussed above. However, if the CN group caused only steric repulsion

with Pd, **PCM1b** and **PCM2b** became less stable than the precursor complexes in which CN took a position distant from Pd. We optimized several possible structures of precursor complex in which CN was more distant from Pd than in **PCM1b** and **PCM2b**. However, **PCM1b** and **PCM2b** are actually more stable than those precursor complexes (their structures are given in the Supporting Information). This means that the CN group would yield some stabilization interaction with Pd in **PCM1b** and **PCM2b**.

In the TS, we must take into consideration the possibility that the TS is stabilized by the interaction of the CN group with Pd (Scheme 1). The similar interaction was proposed as a heteroatom effect in the C–H activation of  $\text{CH}_3\text{CN}$  by ruthenium complexes.<sup>15</sup> To examine this possibility, three orientations of  $\text{CH}_3\text{CN}$  and  $\text{CH}_2(\text{CN})_2$  were optimized without any con-

Scheme 1



straint. In these three TS geometries of the  $\text{CH}_3\text{CN}$  reaction, **TS1a** is the most stable, while **TS1b** is only 0.7 kcal/mol less stable and **TS1c** is 3 kcal/mol less stable than **TS1a**. Because of very small energy difference between **TS1a** and **TS1b**, two reaction courses seem possible; one proceeds through **TS1a**, and the other through **TS1b**. The reaction through **TS1c** is unfavorable because this TS is 3 kcal/mol less stable. In the TS of the C–H activation of  $\text{CH}_2(\text{CN})_2$ , two possible rotation isomers of  $\text{CH}_2(\text{CN})_2$  were optimized, as shown in Figure 2. The other rotation isomer of  $\text{CH}_2(\text{CN})_2$  could not be optimized, since the geometry converged to **TS2a** during the optimization. In those two transition state structures, **TS2a** is 2.8 kcal/mol more stable than **TS2b**. This means that the C–H activation of  $\text{CH}_2(\text{CN})_2$  predominantly takes place through **TS2a**. Here, we will examine whether the Pd–(C≡N) interaction stabilizes the TS. If the CN group did not form a stabilization interaction with Pd, the CN group would take a position distant from Pd to decrease the steric repulsion. However, **TS1a** is actually the most stable, whereas the CN group is closer to Pd in **TS1a** than in **TS1b** and **TS1c**. Similar results are found in the transition state structures of the  $\text{CH}_2(\text{CN})_2$  reaction, as follows: **TS2a** is more stable than **TS2b**, whereas the CN group is closer to Pd in **TS2a** than in **TS2b**. These results suggest that some interaction between Pd and the CN group contributes to the stabilization of the TS, and the stabilization energy is estimated to be about 3 kcal/mol, considering the energy differences between **TS1a** and **TS1c** and between **TS2a** and **TS2b**.

The C–H bond lengthens to 1.56–1.67 Å in the TS of the  $\text{CH}_3\text{CN}$  reaction and 1.56–1.58 Å in the TS of the  $\text{CH}_2(\text{CN})_2$  reaction. Although these distances are considerably shorter than the C–H distance in the TS of the  $\text{CH}_4$  activation,<sup>13b</sup> these distances are much longer than the usual C–H bond (1.09 Å). Moreover, Pd–H and Pd–C distances of these TSs are similar to those of the product, while they are slightly longer than those in the TS of the  $\text{CH}_4$  activation.<sup>13b</sup> Thus, these TSs are characterized to be productlike.

In the products of the  $\text{CH}_3\text{CN}$  reaction, **PRD1b** is the most stable, while **PRD1a** is only 1 kcal/mol less stable and **PRD1c** is 4.2 kcal/mol less stable than **PRD1b**. The most stable **TS1a** leads to the slightly less stable **PRD1a**, and the slightly less stable **TS1b** leads to the most stable **PRD1b**. However, the most unstable **TS1c** leads to the most unstable **PRD1c**. Thus, the former two reaction courses (**TS1a** → **PRD1a** and **TS1b** → **PRD1b**) are possible, while the last one (**TS1c** → **PRD1c**) is unfavorable. In the products of the  $\text{CH}_2(\text{CN})_2$  reaction, **PRD2a** is the most stable, **PRD2c** is 1.2 kcal/mol less stable, and **PRD2b** is 3 kcal/mol less stable than **PRD2a**. The less stable **PRD2b** is produced from the less stable **TS2b**. The reaction through **TS2b** is again unfavorable from the viewpoint of reaction energy.

In all the products, the Pd– $\text{PH}_3(2)$  bond at a position trans to the hydride is about 0.1 Å longer than the Pd– $\text{PH}_3(1)$  bond at a position trans to the alkyl group. The similar geometrical feature is found in  $\text{PdH}(\text{CH}(\text{CN})_2)(\text{PH}_3)_2$ . This Pd– $\text{PH}_3(1)$  bond becomes longer in the order  $\text{PdH}(\text{CH}(\text{CN})_2)(\text{PH}_3)_2 < \text{PdH}(\text{CH}_2\text{CN})(\text{PH}_3)_2 < \text{PdH}(\text{CH}_3)(\text{PH}_3)_2$ . From these results, it should be concluded that *trans*-influence becomes stronger in the order  $\text{CH}(\text{CN})_2 < \text{CH}_2\text{CN} < \text{CH}_3 < \text{H}$  (hydride).

**Geometry Changes in the C–H Activation of  $\text{CH}_3\text{CN}$  and  $\text{CH}_2(\text{CN})_2$  by a Chelate Phosphine Model Complex, Pd(dipe).** Important geometries of precursor complexes, TS's, and products are shown in Figures 3 and 4. **PCM3a** and **PCM4a** involve the  $\eta^1$ -end-on coordination of  $\text{CH}_3\text{CN}$  and  $\text{CH}_2(\text{CN})_2$ . **PCM3b** and **PCM4b** involve  $\eta^2$ -side-on coordination, which are less stable than **PCM3a** and **PCM4a** by 6.2 and 4.1 kcal/mol, respectively. It is noted here that the CN bond slightly lengthens by 0.01–0.02 Å in **PCM3b** and **PCM4b** unlike that in **PCM1b** and **PCM2b**. Although this bond lengthening occurs to a much lesser extent than that in the experimentally isolated  $\eta^2$ -side-on  $\text{CH}_3\text{CN}$  complexes,<sup>23</sup> this bond lengthening would be related to the back-bonding interaction between Pd d and CN  $\pi^*$  orbitals, as will be discussed below. Actually, the Pd–CN distance in **PCM3b** and **PCM4b** is much shorter than that in **PCM1b** and **PCM2b**, and the CN group takes a favorable position for coordination to Pd. **PCM3b** and **PCM4b** are considered to be on the reaction pathway, since the C–H bond takes a position near Pd.

In both C–H activations of  $\text{CH}_3\text{CN}$  and  $\text{CH}_2(\text{CN})_2$ , we examined three kinds of TS's in which the orientations of  $\text{CH}_2\text{CN}$  and  $\text{CH}(\text{CN})_2$  are different (see Figures 3 and 4). In the C–H activation of  $\text{CH}_3\text{CN}$ , **TS3a** is the most stable, **TS3b** is 1.1 kcal/mol less stable, and **TS3c** is 2.6 kcal/mol less stable than **TS3a**. In the C–H activation of  $\text{CH}_2(\text{CN})_2$ , **TS4a** is the most stable, **TS4b** is 2.5 kcal/mol less stable, and **TS4c** is 2.9 kcal/mol less stable than **TS4a**. In these TS structures, the C–H distance is in the range of 1.48–1.60 Å for **TS3a**–**TS3c** and 1.40–1.49 Å for **TS4a**–**TS4c**. These bond distances are ca. 0.1 Å shorter than those in the TS's of the C–H activation of  $\text{CH}_3\text{CN}$  and  $\text{CH}_2(\text{CN})_2$  by  $\text{Pd}(\text{PH}_3)_2$ . The Pd–H and Pd–C distances are only slightly longer than those in the products. These TS's are still considered to be productlike.

In these transition states, a stabilizing interaction between Pd and the CN group is observed as in **TS1a** and **TS2a**. For instance, **TS3c** is the least stable, whereas it seems the most favorable from the steric repulsion. Although **TS4b** is expected to be more favorable than **TS4a** from the steric repulsion, **TS4b** is less stable than **TS4a**. These results clearly indicate that a stabilization interaction exists between Pd and the C≡N group.

In the products, **PRD3b** is the most stable and **TS3b** leading to this product is only 1.1 kcal/mol less stable than **TS3a**. **PRD3a** is only 1.5 kcal/mol less stable than **PRD3b**, while **TS3a** leading to **PRD3a** is the most stable. Thus, these two reaction courses are favorable. The remaining course (**TS3c** → **PRD3c**) seems unfavorable, since both **TS3c** and **PRD3c** are the least stable. In the products of the  $\text{CH}_2(\text{CN})_2$  reaction, **PRD4a** is the most stable, **PRD4b** is 2.8 kcal/mol less stable, and

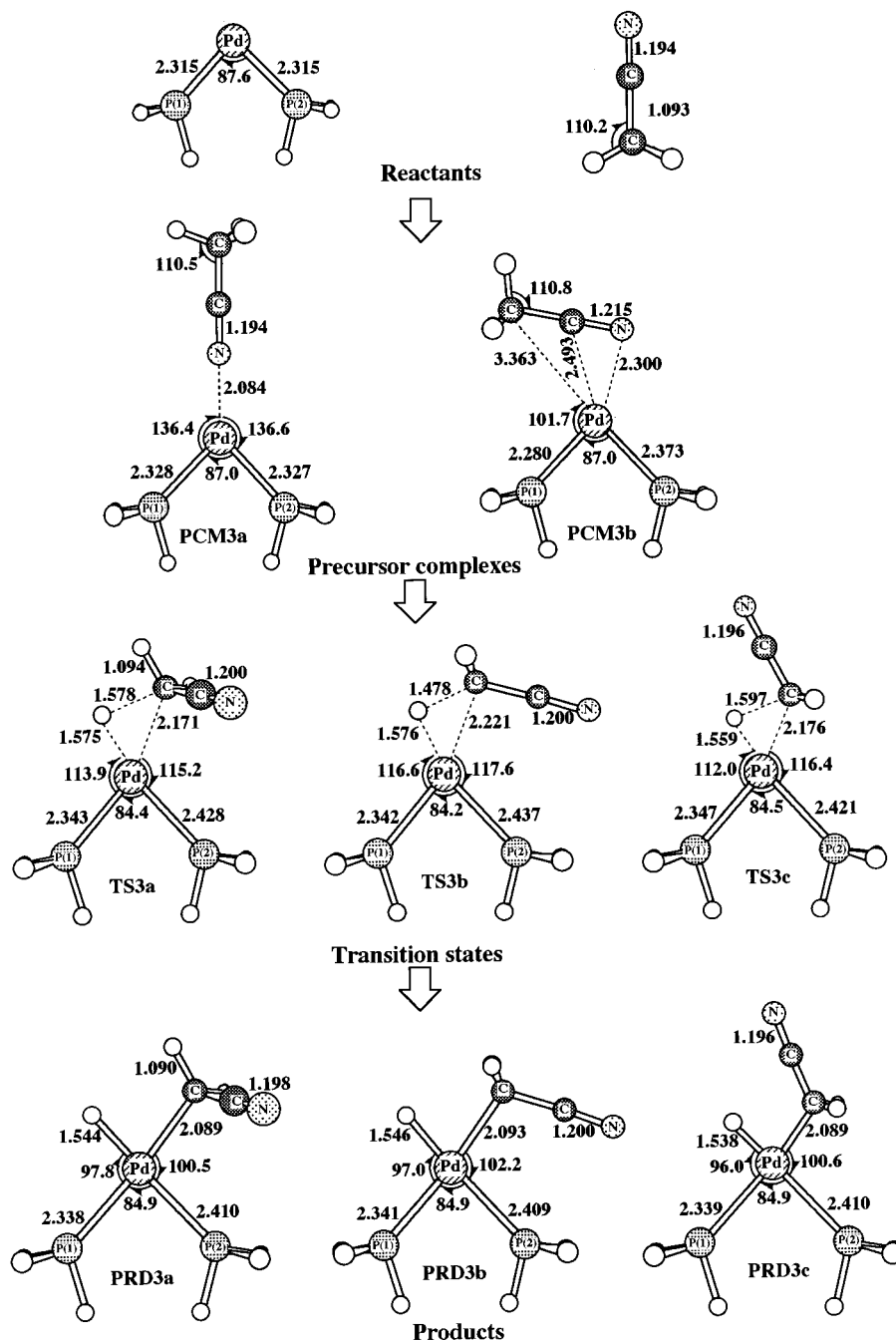


**Figure 3.** Geometry changes in the C–H activation of CH<sub>3</sub>CN by Pd(dipe). Bond lengths are in Å, and bond angles, in deg.

**PRD4c** is 0.6 kcal/mol less stable than **PRD4a**. Thus, the most stable **TS4a** leads to the most stable product **PRD4a**. This reaction course is the most favorable, while the other reaction courses (**TS4b** → **PRD4b** and **TS4c** → **PRD4c**) seem unfavorable because the lesser stabilities of **TS4b** and **TS4c**. In these chelate phosphine models, the Pd–PH<sub>3</sub>(1) distance also becomes longer in the order PdH(CH(CN)<sub>2</sub>)(dipe) < PdH(CH<sub>2</sub>CN)(dipe) < PdH(CH<sub>3</sub>)(dipe) like that in the monodentate phosphine model.

**Geometry Changes in the C–H Activation of CH<sub>4</sub> and CH<sub>2</sub>(CN)<sub>2</sub> by a More Realistic Model Complex, Pd(dppe).** Since the reaction system involving Pd(dppe) and CH<sub>2</sub>(CN)<sub>2</sub> is considerably complex, only the most favorable reaction course corresponding to the course of **TS4a** → **PRD4a** was investigated, as shown

in Figure 5. There are several small differences between the Pd(dppe) and Pd(dipe) reaction systems. In the reactants, Pd(dipe) and Pd(dppe) take almost the same geometry except that the PPdP angle of Pd(dppe) is larger than that of Pd(dipe). Corresponding to this difference, the P–P distance (3.415 Å) of Pd(dppe) is longer than that of Pd(dipe) (3.205 Å). This is probably because a spherical d<sup>10</sup> electron configuration of palladium(0) leads to a nondirectional bonding feature, and therefore, dppe tends to take its equilibrium structure in palladium(0) complexes as follows: the P–P distance is 3.47 Å in the free dppe, and therefore, the PPdP angle must increase to accommodate the rather long P–P distance. In the precursor complexes, the intermolecular distance between Pd and CH<sub>2</sub>(CN)<sub>2</sub> is a little bit longer in **PCM6a** and **PCM6b** than those of **PCM4a**

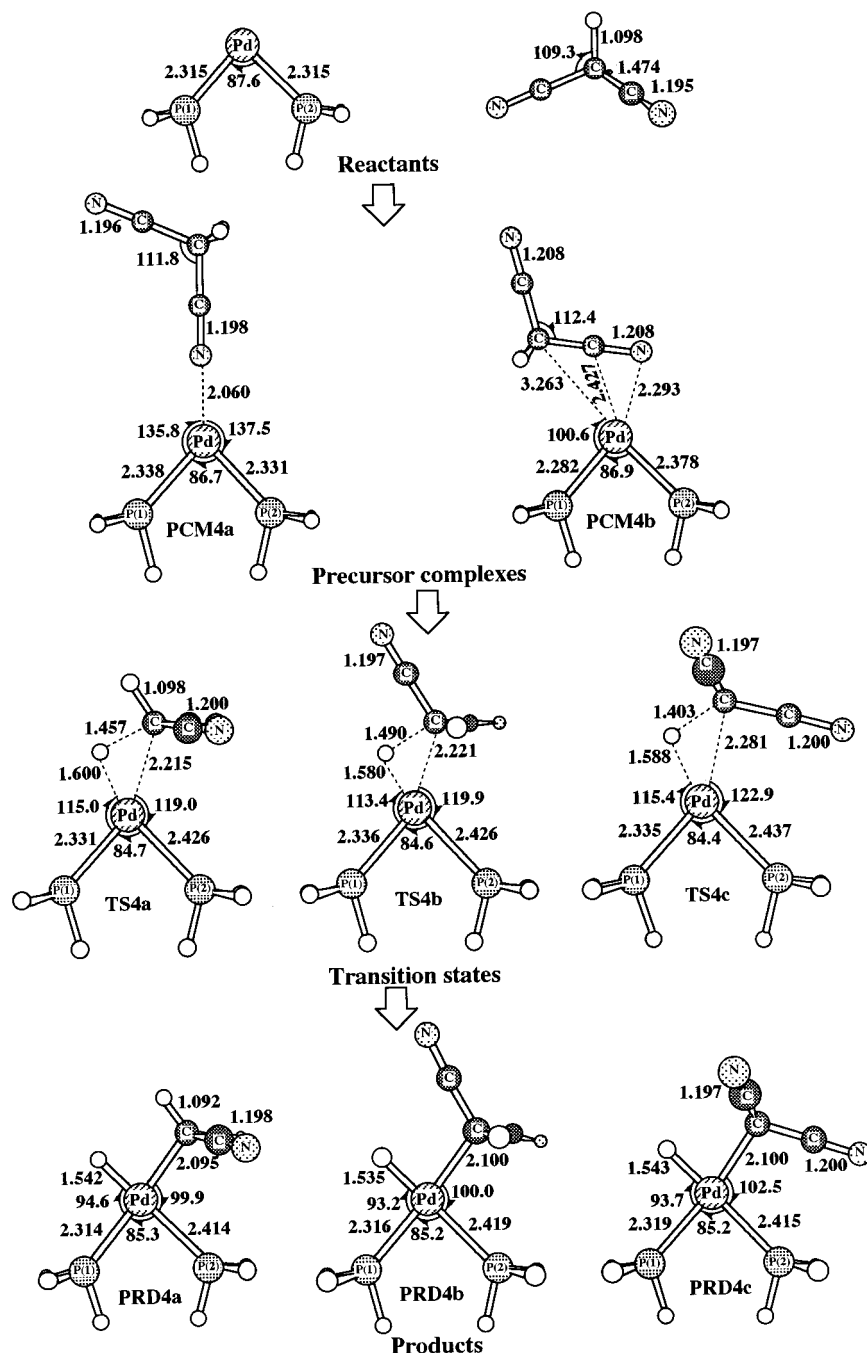


**Figure 4.** Geometry changes in the C-H activation of  $\text{CH}_2(\text{CN})_2$  by  $\text{Pd}(\text{dipe})$ . Bond lengths are in Å, and bond angles, in deg.

and **PCM4b**. In the transition state, the C-H distance of **TS6** is slightly shorter than that of **TS4a**. In the product, the Pd-P distance of **PRD6** is slightly longer than that of **PRD4a**. Although these differences are not significant, it is noted here that the P-P distance of  $\text{Pd}(\text{dipe})$  decreases to 3.23 Å in the product. This is because the palladium atom takes a  $d^8$  electron configuration in the product and the PPdP angle must decrease to ca.  $90^\circ$ . The resultant P-P distance of  $\text{PdH}(\text{CH}(\text{CN})_2)(\text{dipe})$  is almost the same as that of  $\text{PdH}(\text{CH}(\text{CN})_2)(\text{dipe})$ . In other words, the product is well modeled with  $\text{dipe}$ , while the reactant is less appropriately modeled with  $\text{dipe}$  (remember that the P-P distance of  $\text{Pd}(\text{dipe})$  is somewhat shorter than that of  $\text{Pd}(\text{dppe})$ ).

However, geometries of precursor complexes, transition states, and products of the  $\text{Pd}(\text{dipe})$  reaction system

resemble well those of the  $\text{Pd}(\text{dppe})$  system, despite the above-mentioned small differences. For instance, the Pd-P(1) bond at a *trans*-position of the alkyl ligand is longer than the Pd-P(2) bond at a *trans*-position of hydride in both **PRD6** and **PRD4a**. This means that hydride and alkyl ligands exhibit the *trans*-influence in the  $\text{Pd}(\text{dipe})$  system similarly to those in the  $\text{Pd}(\text{dppe})$  system. In conclusion,  $\text{Pd}(\text{dipe})$  is not considered an unreasonable model.

**Energy Changes in the C-H Activation Reaction.** The binding energy (BE), the activation energy ( $E_a$ ), and the reaction energy ( $\Delta E$ ) are calculated with HF-MP4SDQ methods, where BE is the stabilization energy of precursor complex relative to the sum of the reactants,  $E_a$  is the energy difference between TS and the precursor complex on the reaction pathway, and  $\Delta E$

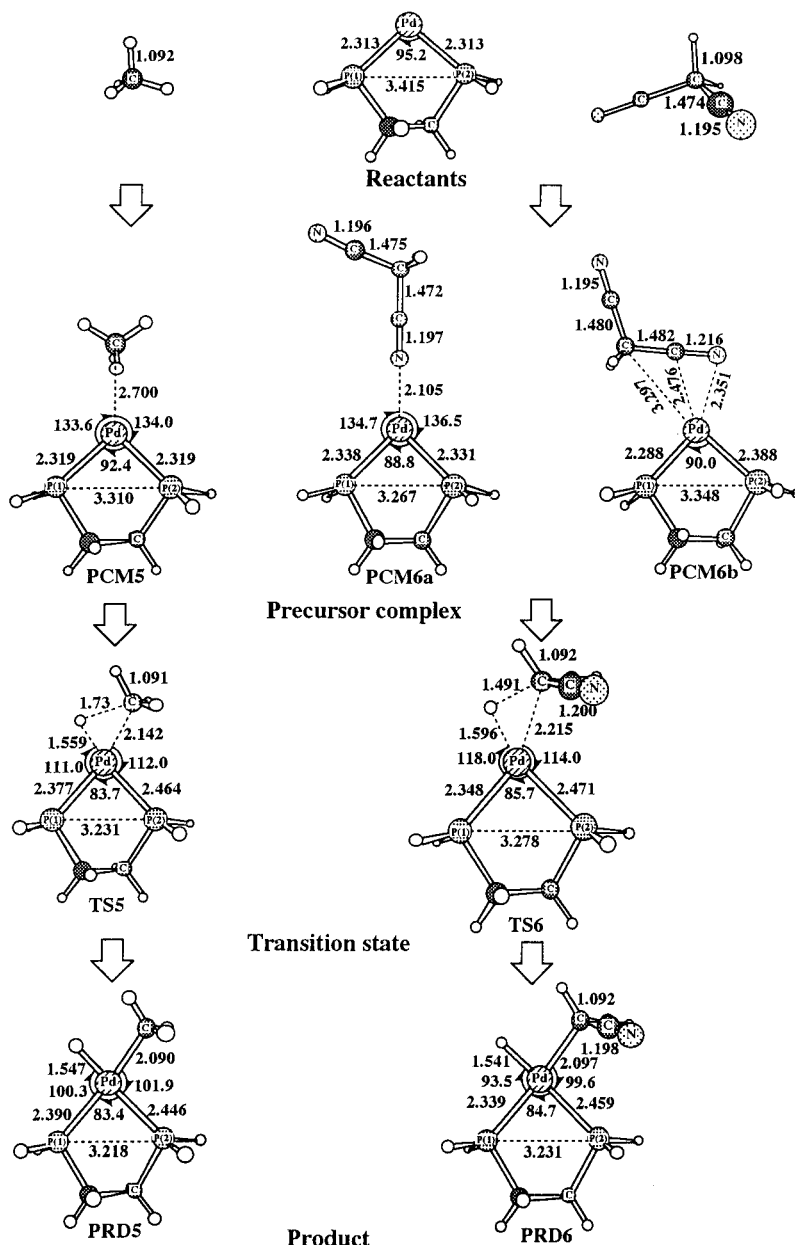


**Figure 5.** Geometry changes in the C–H activation of CH<sub>4</sub> and CH<sub>2</sub>(CN)<sub>2</sub> by Pd(dpe). Bond lengths are in Å, and bond angles, in deg.

**Table 1. Electron-Correlation Effects on BE,<sup>a</sup> E<sub>a</sub>,<sup>b</sup> and ΔE<sup>c</sup> (kcal mol<sup>-1</sup>) in the C–H Oxidative Addition of CH<sub>2</sub>(CN)<sub>2</sub> to Pd(PH<sub>3</sub>)<sub>2</sub> and Pd(dipe)<sup>d</sup>**

	Pd(PH <sub>3</sub> ) <sub>2</sub> + CH <sub>2</sub> (CN) <sub>2</sub>			Pd(dipe) + CH <sub>2</sub> (CN) <sub>2</sub>		
	BE	E <sub>a</sub>	ΔE	BE	E <sub>a</sub>	ΔE
HF	-0.2	42.3	25.6	-0.3	24.7	5.8
MP2	-6.4	20.4	6.4	-20.6	15.3	-15.6
MP3	-4.9	27.0	8.4	-13.0	16.8	-12.4
MP4(DQ)	-4.9	25.8	10.3	-15.5	17.2	-11.6
MP4(SDQ)	-5.7	25.1	10.8	-18.1	18.0	-10.8

<sup>a</sup> BE = E<sub>t</sub> (precursor complex) – E<sub>t</sub> (sum of reactants), where the precursor complex on the reaction course was taken. <sup>b</sup> E<sub>a</sub> = E<sub>t</sub>(TS) – E<sub>t</sub>(precursor complex). <sup>c</sup> ΔE = E<sub>t</sub>(product) – E<sub>t</sub>(sum of reactants). <sup>d</sup> Calculated for reaction courses TS2a → PRD2a and TS4a → PRD4a.

is the energy difference between the product and the sum of reactants.

As shown in Table 1, BE, E<sub>a</sub>, and ΔE slightly fluctuate upon going to MP4SDQ from MP3 to a similar extent to those values calculated in the C–H activation of CH<sub>4</sub>

by Pt(PH<sub>3</sub>)<sub>2</sub> and Pd(PH<sub>3</sub>)<sub>2</sub>, which was theoretically investigated in our previous work.<sup>13b</sup> In our previous work, we also ascertained that a single reference wave function is useful even for the TS and the MP4SDQ method yields almost the same BE, E<sub>a</sub>, and ΔE values as those of the coupled cluster with a double substitution calculation.<sup>13b</sup> Thus, the MP4SDQ method is considered reliable in the reaction systems investigated here.

BE, E<sub>a</sub>, and ΔE values calculated with the MP4SDQ method are compared among various reaction systems in Table 2, where BE and E<sub>a</sub> values after correction of the basis set superposition error (BSSE) are given in parentheses.

The BE value varies considerably among methane and methane derivatives involving the CN group. In Pd(PH<sub>3</sub>)<sub>2</sub>, CH<sub>3</sub>CN and CH<sub>2</sub>(CN)<sub>2</sub> coordinations yield 4–5 kcal/mol of BE, while most of them arise from BSSE. In Pd(dipe), however, CH<sub>3</sub>CN and CH<sub>2</sub>(CN)<sub>2</sub> coordinations yield considerably larger BE values of 22



**Table 2.** BE,  $E_a$ , and  $\Delta E$  for Various Reaction Systems (kcal mol<sup>-1</sup> at the MP4SDQ Level)

system	BE <sub>1</sub> <sup>a</sup>	BE <sub>2</sub> <sup>b</sup>	$E_a$	$\Delta E$
Pd(PH <sub>3</sub> ) <sub>2</sub> + CH <sub>4</sub> <sup>c</sup>		-0.7 (-0.1) <sup>d</sup>	36.9 (44.2) <sup>d</sup>	34.1
Pd(PH <sub>3</sub> ) <sub>2</sub> + CH <sub>3</sub> CN				
TS1a → PRD1a	-4.7	-4.2 (-1.8) <sup>d</sup>	32.6 (38.6) <sup>d</sup>	22.2
TS1b → PRD1b			31.9	23.2
TS1c → PRD1c			34.9	26.3
Pd(PH <sub>3</sub> ) <sub>2</sub> + CH <sub>2</sub> (CN) <sub>2</sub>				
TS2a → PRD2a	-4.4	-5.7 (-2.4) <sup>d</sup>	25.1 (31.8) <sup>d</sup>	10.8
TS2b → PRD2b			27.9	13.7
Pd(dipe) + CH <sub>4</sub> <sup>c</sup>		-7.7 (-3.6) <sup>d</sup>	22.1 (25.6) <sup>d</sup>	11.7
Pd(dipe) + CH <sub>3</sub> CN				
TS3a → PRD3a	-22.3	-16.1 (-10.0) <sup>d</sup>	24.1 (25.4) <sup>d</sup>	-0.1
TS3b → PRD3b			23.2	1.4
TS3c → PRD3c			25.7	4.4
Pd(dipe) + CH <sub>2</sub> (CN) <sub>2</sub>				
TS4a → PRD4a	-22.2	-18.1 (-11.5) <sup>d</sup>	18.0 (20.8) <sup>d</sup>	-10.8
TS4b → PRD4b			20.5	-8.0
TS4c → PRD4c			21.0	-10.2
Pd(dppe) + CH <sub>4</sub>		-5.1	26.7	19.8
Pd(dppe) + CH <sub>2</sub> (CN) <sub>2</sub>				
TS6 → PRD6	-16.7	-13.5 (-7.1) <sup>d</sup>	19.3 (22.6) <sup>d</sup>	-6.0

<sup>a</sup> The  $\eta^1$ -end-on coordination structure of the CN group. <sup>b</sup> The  $\eta^2$ -side-on coordination structure of the CN group. <sup>c</sup> Reference 13b. <sup>d</sup> The basis set superposition error was corrected at the MP4SDQ level with the counter-poise method.<sup>24</sup>

kcal/mol for the  $\eta^1$ -end-on coordination structure and 16–18 kcal/mol for  $\eta^2$ -side-on coordination structure. The BE of the Pd(dppe) system is about 4–5 kcal/mol smaller than the BE of the Pd(dipe) system. Even after BSSE correction, BE of the  $\eta^2$ -side-on coordination structure is about 10–12 kcal/mol for the Pd(dipe) system and 7 kcal/mol for the Pd(dppe) system. We must remember here that Boys method overestimates BSSE. Thus,  $\eta^2$ -side-on coordination complexes such as **PCM3b**, **PCM4b**, and **PCM6b** are considered as an intermediates.

The  $E_a$  value considerably decreases by introduction of CN, in the order CH<sub>4</sub> > CH<sub>3</sub>CN > CH<sub>2</sub>(CN)<sub>2</sub> for Pd(PH<sub>3</sub>)<sub>2</sub>, CH<sub>3</sub>CN > CH<sub>4</sub> > CH<sub>2</sub>(CN)<sub>2</sub> for Pd(dipe), and CH<sub>4</sub> ≫ CH<sub>2</sub>(CN)<sub>2</sub> for Pd(dppe) (Table 2). Here, we should mention that the C–H activation of CH<sub>3</sub>CN by Pd(dipe) requires a slightly higher  $E_a$  value than that of CH<sub>4</sub> by Pd(dipe). This is because the precursor complex, Pd(dipe)(CH<sub>3</sub>CN) **PCM3b**, is much more stable than the precursor complex Pd(dipe)(CH<sub>4</sub>), and the stabilization of **PCM3b** is greater than that of **TS3a**. The lowest  $E_a$  value of 18 kcal/mol was calculated in the C–H activation of CH<sub>2</sub>(CN)<sub>2</sub> by Pd(dipe). A similar  $E_a$  value was also calculated in the C–H activation of CH<sub>2</sub>(CN)<sub>2</sub> by Pd(dppe). Thus, the  $E_a$  value is considered reliable even in the simple dipe model. These moderately low  $E_a$  values suggest that the C–H activation of CH<sub>2</sub>(CN)<sub>2</sub> by Pd(chelate phosphine) easily occurs. The reason that Pd(dipe) and Pd(dppe) can more easily perform the C–H activation than Pd(PH<sub>3</sub>)<sub>2</sub> was investigated previously.<sup>13b</sup> The discussion is omitted here.

The reaction energy also decreases very much by introduction of CN in the order CH<sub>4</sub> > CH<sub>3</sub>CN > CH<sub>2</sub>(CN)<sub>2</sub> for both Pd(PH<sub>3</sub>)<sub>2</sub> and Pd(dipe) and CH<sub>4</sub> ≫ CH<sub>2</sub>(CN)<sub>2</sub> for Pd(dppe). It is noted that the C–H activation of CH<sub>2</sub>(CN)<sub>2</sub> by Pd(dipe) and Pd(dppe) is exothermic, whereas the other reactions are endothermic. This means that the C–H activation requires the higher barrier than the reverse C–H coupling reaction except for the C–H activation of CH<sub>2</sub>(CN)<sub>2</sub> by Pd(dipe) and Pd(dppe): For instance, C–H activation of CH<sub>2</sub>(CN)<sub>2</sub> by

Pd(PH<sub>3</sub>)<sub>2</sub> requires an activation barrier of 25 kcal/mol, but the reverse reaction needs a lower activation barrier of 14 kcal/mol. In the C–H activation of CH<sub>2</sub>(CN)<sub>2</sub> by Pd(dipe) and Pd(dppe), however, the situation completely changes, as follows: the reverse C–H coupling reaction requires a higher activation barrier than C–H activation. Thus, C–H activation easily proceeds in these reaction systems.

Here, we mention that the Pd(dipe) reaction is more exothermic than the Pd(dppe) reaction. This is because the fixed P–P distance of the Pd(dipe) system somewhat deviates from that of the Pd(dppe) system in the reactant but only slightly shifts in the product (see above); in other words, the reactant side of the Pd(dipe) reaction system is calculated to be less stable than the more realistic Pd(dppe) reactant system, which leads to an overestimated exothermicity of the Pd(dipe) reaction system. On the other hand, the  $E_a$  value is similar in Pd(dipe) and Pd(dppe) systems (vide supra), because the P–P distance of dppe little changes upon going to **TS6** from **PCM6b** (note that  $E_a$  is an energy difference between **TS6** and **PCM6b**).

From the above results, it should be reasonably concluded that two conditions must be satisfied to easily perform the sp<sup>3</sup> C–H activation by a palladium(0) complex; one is introduction of two CN groups on the sp<sup>3</sup> carbon atom, and the other is use of a chelate phosphine. The reaction of Yamamoto et al.<sup>14</sup> certainly satisfied these two conditions; for instance, either two CN groups or CN and CO<sub>2</sub>Et groups were introduced on the sp<sup>3</sup> carbon atom, and a chelate phosphine was used. Thus, the present computational results provide a theoretical support that the sp<sup>3</sup> C–H activation of methane derivatives can be carried out even by a palladium(0) complex, if an appropriate chelate phosphine is used as a ligand and electron-withdrawing groups are introduced on the sp<sup>3</sup> carbon atom. Of course, these two conditions are not absolutely necessary. The catalytic reaction involving the C–H activation by a palladium complex can be constructed, if different conditions are satisfied. As described above, the C–H activation of CH<sub>2</sub>(CN)<sub>2</sub> by Pd(PH<sub>3</sub>)<sub>2</sub> can occur with a barrier of 25 kcal/mol. This barrier is not high very much, but the reverse C–H coupling reaction takes place with a lower barrier of 14 kcal/mol. If the successive step after the C–H activation more easily proceeds than the C–H coupling reaction, the catalytic reaction might proceed. Certainly, palladium-catalyzed hydrocarbonation of methylenecyclopropane was recently carried out by Yamamoto et al. at rather high temperature (100 °C), where Pd(PPh<sub>3</sub>)<sub>4</sub> was used as a catalyst.<sup>25</sup> The success of this catalytic reaction is easily understood, if we suppose that the high temperature is necessary to perform the C–H activation by Pd(PPh<sub>3</sub>)<sub>4</sub> and methylenecyclopropane more easily reacts with the palladium(II) alkyl hydride complex than the reverse C–H coupling reaction.

**Why Does the Electron-Withdrawing Group Accelerate C–H Activation?** Natural orbital population changes<sup>26</sup> in the C–H activation by Pd(dipe) are shown

(24) Boys, S. F.; Bernardi, F. *Mol. Phys.* **1970**, *19*, 553.

(25) Yamamoto, Y. Private communication. Tsukada, N.; Shibuya, A.; Nakamura, I.; Yamamoto, Y. *J. Am. Chem. Soc.* **1997**, *119*, 8123.

(26) Reed, A. E.; Curtiss, L. A.; Weinhold, F. *Chem. Rev.* **1988**, *88*, 849 and references therein.

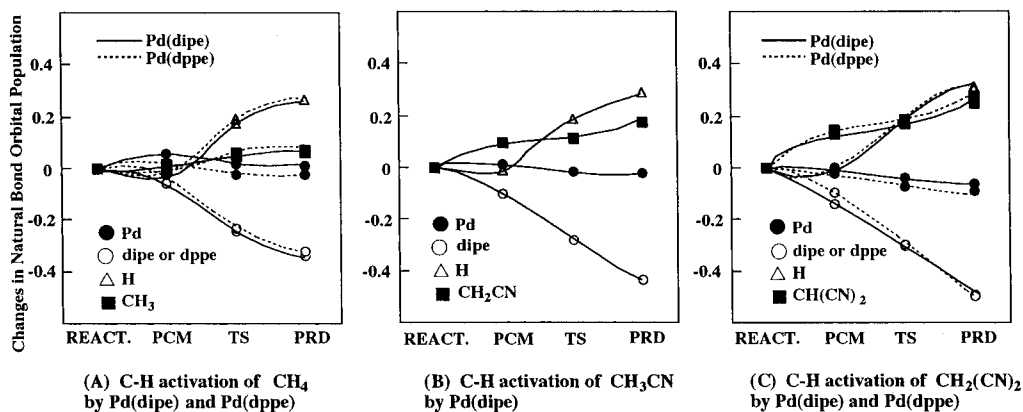


**Figure 6.** Natural bond orbital population changes in the C–H activation of CH<sub>4</sub>, CH<sub>3</sub>CN, and CH<sub>2</sub>(CN)<sub>2</sub> by Pd(dipe) and Pd(dppe). A positive value represents an increase in population. Dotted lines represent population changes in the Pd(dppe) system.

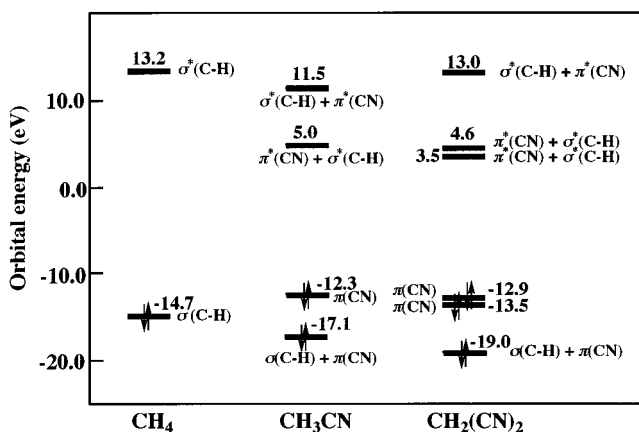
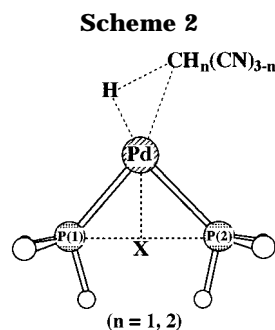


**Figure 7.** Frontier orbital energies of CH<sub>4</sub>, CH<sub>3</sub>CN, and CH<sub>2</sub>(CN)<sub>2</sub>.

in Figure 6. Almost the same population changes occur in Pd(dppe) systems, as shown by dotted lines in Figure 6. Apparently, the electron populations of H and alkyl (CH<sub>3</sub>, CH<sub>2</sub>CN, or CH(CN)<sub>2</sub>) moieties substantially increase and the Pd atomic population substantially decreases, as the reaction proceeds. These changes are consistent with our understanding that this type of reaction might be considered as an oxidative addition. It should be noted that the electron population of the CH(CN)<sub>2</sub> moiety increases the most (by ca. 0.17 e), that of the CH<sub>2</sub>CN moiety increases the next (by ca. 0.11 e), and that of the CH<sub>3</sub> moiety increases the least (by ca. 0.05 e) at the TS, while the H atomic population similarly increases in all three reaction systems. These results suggest that the electron-withdrawing CN group enhances the charge-transfer interaction from Pd to the alkyl group.

In Figure 7, frontier orbital energies of CH<sub>4</sub>, CH<sub>3</sub>CN, and CH<sub>2</sub>(CN)<sub>2</sub> are shown. Although CH<sub>4</sub> has its C–H  $\sigma$  orbital at a very low energy and its C–H  $\sigma^*$  orbital at a very high energy, CH<sub>3</sub>CN and CH<sub>2</sub>(CN)<sub>2</sub> have  $\pi$  orbitals of the C≡N triple bond at a higher energy than the C–H  $\sigma$  orbital and  $\pi^*$  orbitals of the C≡N triple bond at a considerably lower energy than the C–H  $\sigma^*$  orbital. Interestingly, the C–H  $\sigma^*$  orbital mixes into the  $\pi^*$  orbital, as shown in Scheme 2 (we represent this orbital as  $\pi^*(\text{CN}) + \sigma^*(\text{CH})$ , hereafter). Because this  $\pi^*(\text{CN}) + \sigma^*(\text{CH})$  orbital is at a lower energy than the CH<sub>4</sub>  $\sigma^*$  orbital, the charge transfer from Pd to CH<sub>3</sub>CN



and CH<sub>2</sub>(CN)<sub>2</sub> much more easily occurs than that to the CH<sub>4</sub>  $\sigma^*$  orbital. Moreover, such charge-transfer interaction weakens the C–H bond and stabilizes the transition state, to accelerate the C–H activation. This is the origin of the stabilization interaction between Pd and the CN group. To form this interaction, the CN group takes a position near Pd in the TS and lowers the activation energy, as discussed above. This result also suggests that C–H activation is accelerated when the electron-withdrawing group possesses the  $\pi^*$  orbital into which the C–H  $\sigma^*$  orbital can mix. In the palladium-catalyzed addition of activated methylene and methyne to allene, not only CN but also COOEt is introduced on the carbon atom.<sup>14</sup> The COOEt group is also expected to play a role similar to that of the CN group, since the COOEt group has the  $\pi^*$  orbital. The higher reactivities of Pd(dipe) and Pd(dppe) compared to that of Pd(PH<sub>3</sub>)<sub>2</sub> are also interpreted in terms of this charge-transfer interaction. As previously investigated,<sup>13b, 27</sup> the Pd  $d_{\pi}$  orbital of Pd(dipe) and Pd(dppe) is at a higher energy than that of Pd(PH<sub>3</sub>)<sub>2</sub>.<sup>13b, 27, 28</sup> Thus, Pd(dipe) and Pd(dppe) can form the stronger charge-transfer interaction than Pd(PH<sub>3</sub>)<sub>2</sub>, which leads to the higher reactivity.

We should mention here the population change at the precursor complexes. As clearly shown in Figure 6, the populations of methane and methane derivatives increase in the order CH<sub>4</sub> (0.017 e) < CH<sub>3</sub>CN (0.096 e) < CH<sub>2</sub>(CN)<sub>2</sub> (0.149 e) in the precursor complexes of Pd(dipe) and CH<sub>4</sub> (–0.005 e) < CH<sub>2</sub>(CN)<sub>2</sub> (0.129 e) in the precursor complexes of Pd(dppe), where the positive numbers in parentheses represent the increase in NBO

(27) Albright, T. A.; Hoffmann, R.; Thibault, J. C.; Thorn, D. L. *J. Am. Chem. Soc.* **1979**, *101*, 3801.

(28) The  $d_{\pi}$  orbital is at –7.1 and –9.6 eV in Pd(dppe) and Pd(PH<sub>3</sub>)<sub>2</sub>, respectively.

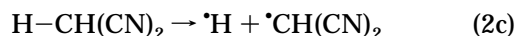
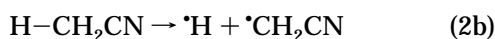
**Table 3. C–H and Pd–Alkyl Bond Energies (kcal/mol)**

systems	bond energy	MP2	MP3	MP4(DQ)	MP4(SDQ)
CH <sub>4</sub>	<i>E</i> (H–CH <sub>3</sub> )	107.9	108.6	108.6	108.6
CH <sub>3</sub> CN	<i>E</i> (H–CH <sub>2</sub> CN)	111.7	105.8	107.2	106.4
CH <sub>2</sub> (CN) <sub>2</sub>	<i>E</i> [H–CH(CN) <sub>2</sub> ]	115.5	102.3	105.7	104.4
<i>cis</i> -PdH <sub>2</sub> (PH <sub>3</sub> ) <sub>2</sub>	<i>E</i> (Pd–H)	50.1	51.6	52.7	53.3
<i>cis</i> -Pd(H)(CH <sub>3</sub> )(PH <sub>3</sub> ) <sub>2</sub>	<i>E</i> (Pd–CH <sub>3</sub> )	26.0	23.7	22.1	21.2
<i>cis</i> -Pd(H)(CH <sub>2</sub> CN)(PH <sub>3</sub> ) <sub>2</sub> <sup>a</sup>	<i>E</i> (Pd–CH <sub>2</sub> CN)	42.6	34.4	32.9	30.9
<i>cis</i> -Pd(H)[CH(CN) <sub>2</sub> ](PH <sub>3</sub> ) <sub>2</sub> <sup>a</sup>	<i>E</i> [Pd–CH(CN) <sub>2</sub> ]	58.2	42.4	42.7	40.1
<i>cis</i> -PdH <sub>2</sub> (dipe)	<i>E</i> (Pd–H)	60.0	59.8	61.2	61.7
<i>cis</i> -Pd(H)(CH <sub>3</sub> )(dipe)	<i>E</i> (Pd–CH <sub>3</sub> )	40.1	37.0	35.9	35.2
<i>cis</i> -Pd(H)(CH <sub>2</sub> CN)(dipe) <sup>a</sup>	<i>E</i> (Pd–CH <sub>2</sub> CN)	56.6	47.6	46.6	44.7
<i>cis</i> -Pd(H)[CH(CN) <sub>2</sub> ](dipe) <sup>a</sup>	<i>E</i> [Pd–CH(CN) <sub>2</sub> ]	71.4	55.0	55.8	53.2
<i>cis</i> -PdH <sub>2</sub> (dppe)	<i>E</i> (Pd–H)	56.9	57.3	58.6	58.9
<i>cis</i> -Pd(H)(CH <sub>3</sub> )(dppe)	<i>E</i> (Pd–CH <sub>3</sub> )	35.0	32.9	31.3	30.0
<i>cis</i> -Pd(H)[CH(CN) <sub>2</sub> ](dppe) <sup>a</sup>	<i>E</i> [Pd–CH(CN) <sub>2</sub> ]	69.5	54.3	54.4	51.1

<sup>a</sup> The most stable geometries were taken for calculations.

population. A similar but smaller increase of NBO population is also observed in the precursor complexes of Pd(PH<sub>3</sub>)<sub>2</sub>; CH<sub>4</sub> (~0 e) < CH<sub>3</sub>CN (0.015 e) < CH<sub>2</sub>(CN)<sub>2</sub> (0.028 e). These results indicate that (1) the introduction of the CN group enhances the charge transfer from Pd to CH<sub>3</sub>CN and CH<sub>2</sub>(CN)<sub>2</sub>, (2) the CN π\* orbital participates in the back-bonding interaction with Pd, and (3) the back-bonding interaction is stronger in the precursor complexes of Pd(dipe) and Pd(dppe) than in those of Pd(PH<sub>3</sub>)<sub>2</sub>, because the chelate phosphine destabilizes the Pd d<sub>π</sub> orbital more than the monodentate phosphine.<sup>13b,27</sup>

**Why Does the Endothermicity Decrease by Introduction of CN?** As described above, the endothermicity of the C–H activation decreases very much by introduction of the CN group. We must examine two factors to understand this result: One is the C–H bond strength, and the other is the Pd–CH<sub>2</sub>CN and Pd–CH(CN)<sub>2</sub> bond strengths. We evaluated the C–H bond energy by considering the following reactions:



The Pd–alkyl bond energy was evaluated through two steps: First, the Pd–H bond energy was evaluated with eqs 3a,b. Second, the sum of Pd–H and Pd–alkyl bond



energies was estimated with eqs 1a–1e. Then, the Pd–alkyl bond energy was obtained by subtracting the Pd–H bond energy from the sum. As listed in Table 3, the C–H and Pd–alkyl bonds become stronger by introduction of the CN group; in particular, it should be noted that introduction of one CN group strengthens the Pd–alkyl bond by ca. 16 kcal/mol and the C–H bond by ca. 4 kcal/mol. Since the Pd–alkyl bond strengthens more than does the C–H bond upon introduction of the CN group, the C–H activation becomes less endothermic (or more exothermic) by introduction of the CN group.

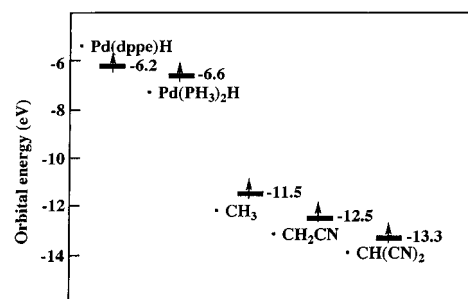
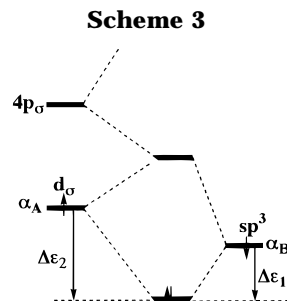


**Figure 8.** The d<sub>σ</sub> orbital energies of Pd(PH<sub>3</sub>)<sub>2</sub>H and Pd(dppe)H (doublet states) and sp<sup>3</sup> orbital energies of the  $\cdot\text{CH}_3$ ,  $\cdot\text{CH}_2\text{CN}$ , and  $\cdot\text{CH(CN)}_2$  radicals.



Why does the Pd–alkyl bond become stronger in the order CH<sub>3</sub> < CH<sub>2</sub>CN < CH(CN)<sub>2</sub>? As shown in Figure 8, the alkyl sp<sup>3</sup> orbital lowers in energy in the order  $\cdot\text{CH}_3 > \cdot\text{CH}_2\text{CN} > \cdot\text{CH(CN)}_2$ . This sp<sup>3</sup> orbital energy is easily related to the Pd–alkyl bond energy through a simple perturbation, as follows: In general, the metal d orbital is at a much higher energy than the ligand orbital. Actually, the alkyl sp<sup>3</sup> orbital was calculated around –11 to –13 eV, and the d<sub>σ</sub> orbital was calculated at –6.6 eV in PdH(PH<sub>3</sub>)<sub>2</sub> and –6.2 eV in PdH(dppe) (Figure 8), where the geometries of PdH(PH<sub>3</sub>)<sub>2</sub> and PdH(dppe) were taken to be the same as that of **PRD2a** and **PRD6**, respectively.<sup>29</sup> As shown in Scheme 3, the bonding and antibonding orbitals are formed from the metal d<sub>σ</sub> orbital and the alkyl radical sp<sup>3</sup> orbital (hereafter, α<sub>A</sub> and α<sub>B</sub> represent the metal d<sub>σ</sub> and alkyl sp<sup>3</sup> orbital energies, respectively). When the term of α<sub>A</sub> – α<sub>B</sub> is larger than the resonance integral β between metal d and alkyl sp<sup>3</sup> orbitals, the stabilization energies

(29) Even when the geometry of PdH(PH<sub>3</sub>)<sub>2</sub> was taken to be the same as that of **PRD4a**, the d orbital energy was almost the same (the difference is about 0.1 eV).

( $\Delta\epsilon_1$  and  $\Delta\epsilon_2$ ) relative to  $\alpha_B$  and  $\alpha_A$  are represented with eqs 4a,b, respectively (see Scheme 3 for  $\Delta\epsilon_1$  and  $\Delta\epsilon_2$ ).

$$\Delta\epsilon_1 = \frac{\beta^2}{\alpha_A - \alpha_B} \quad (4a)$$

$$\Delta\epsilon_2 = \alpha_A - \alpha_B + \frac{\beta^2}{\alpha_A - \alpha_B} \quad (4b)$$

$$\Delta\epsilon_t = \Delta\epsilon_1 + \Delta\epsilon_2 = \alpha_A - \alpha_B + \frac{2\beta^2}{\alpha_A - \alpha_B} \quad (4c)$$

As well-known,  $\Delta\epsilon_1$  increases with a decrease of  $\alpha_A - \alpha_B$ , while  $\Delta\epsilon_2$  becomes larger with an increase of  $\alpha_A - \alpha_B$  (note that  $\alpha_A - \alpha_B$  is larger than  $|\beta|$ ). The total electronic stabilization energy  $\Delta\epsilon_t$  is given by a sum of  $\Delta\epsilon_1$  and  $\Delta\epsilon_2$ . The first term ( $\alpha_A - \alpha_B$ ) of eq 4c is predominant and  $\Delta\epsilon_t$  increases with an increase of  $\alpha_A - \alpha_B$  when  $\alpha_A - \alpha_B$  is larger than  $\sqrt{2}|\beta|$ . Since  $\alpha_A - \alpha_B$  is significantly large (5–6 eV) here, this condition would be reasonably satisfied. As shown in Figure 8, the  $sp^3$  orbital of the alkyl group lowers in energy in the order  $\cdot\text{CH}_3 > \cdot\text{CH}_2\text{CN} > \cdot\text{CH}(\text{CN})_2$  and the Pd 4d orbital lies at a higher energy than those  $sp^3$  orbitals. Thus, the stabilization energy by the Pd–alkyl bond formation increases in the order  $\text{CH}_3 < \text{CH}_2\text{CN} < \text{CH}(\text{CN})_2$ . This is a main reason that the Pd–alkyl bond becomes stronger by introduction of the electron-withdrawing CN group, i.e., in the order  $\text{Pd}-\text{CH}_3 < \text{Pd}-\text{CH}_2\text{CN} < \text{Pd}-\text{CH}(\text{CN})_2$ . The above discussion is simple, but some essential features would be involved.

#### **Trans-Influence of $\text{CH}_3$ , $\text{CH}_2\text{CN}$ , and $\text{CH}(\text{CN})_2$ .**

At the end of this discussion, we need to mention the *trans*-influence, since the Pd–alkyl bond strength is not related to the strength of the *trans*-influence, as follows: The *trans*-influence strengthens in the order  $-\text{CH}(\text{CN})_2 < -\text{CH}_2\text{CN} < -\text{CH}_3$  (vide supra). This order is the reverse of the order of Pd–alkyl bond energy. This is surprising because we might expect that the strong bond weakens the other bond. As discussed above, the  $sp^3$  orbital energy becomes higher in the order  $\cdot\text{CH}(\text{CN})_2 < \cdot\text{CH}_2\text{CN} < \cdot\text{CH}_3$ . When the  $sp^3$  orbital rises in energy, the  $d_\sigma$ – $sp^3$  antibonding orbital moves upward in energy, as shown in Scheme 3, and the other ligand becomes difficult to form the dative bond with the  $d_\sigma$ – $sp^3$  antibonding orbital. This means that the *trans*-influence becomes stronger as the  $sp^3$  orbital of alkyl group rises in energy, i.e., in the order  $\text{CH}(\text{CN})_2 < \text{CH}_2\text{CN} < \text{CH}_3$ . In conclusion, the Pd–alkyl bond becomes stronger when the alkyl  $sp^3$  orbital lowers in energy, while the *trans*-influence of alkyl ligand becomes stronger when the alkyl  $sp^3$  orbital energy rises in energy. Thus, the strong Pd–alkyl bond exhibits a weak *trans*-influ-

ence. This unexpected result is reasonably understood by considering the interaction of Scheme 3.

### Conclusions

In this work, the C–H activation of methane derivatives by palladium(0) complexes was theoretically investigated with ab initio MO/MP2–MP4SDQ methods. Although C–H activation becomes easier by introduction of electron-withdrawing CN group on the  $sp^3$  carbon atom, C–H activation by a palladium(0) monodentate phosphine model complex is still not easy. However, the C–H activation of  $\text{CH}_2(\text{CN})_2$  easily occurs with a palladium bidentate phosphine model complex, Pd(dipe) and Pd(dppe). Thus, we propose two conditions under which the C–H activation by a palladium(0) complex can take place easily: One is the introduction of two CN groups on the  $sp^3$  carbon atom, and the other is use of a chelate phosphine as a ligand. Actually, a chelate phosphine was used and two electron-withdrawing groups (CN or  $\text{CO}_2\text{Et}$ ) were introduced on the  $sp^3$  carbon atom in the Pd-catalyzed addition of activated methyne and methylene to allene, in which the C–H activation of methane derivatives by a palladium(0) complexes was involved as a key step.<sup>14</sup>

Roles of electron-withdrawing groups are investigated in detail. At the transition state, the CN  $\pi^*$  orbital enhances the charge-transfer interaction from Pd 4d to the C–H  $\sigma^*$  orbital, since the CN  $\pi^*$  orbital lies at a lower energy than the C–H  $\sigma^*$  orbital. This CN  $\pi^*$  orbital undergoes C–H  $\sigma^*$  orbital mixing. Thus, this charge-transfer interaction not only stabilizes the transition state but also weakens the C–H bond and accelerates the C–H bond breaking. In the product, the electron-withdrawing CN group stabilizes the Pd–alkyl bond. In fact, C–H activation of  $\text{CH}_2(\text{CN})_2$  by Pd(dipe) and Pd(dppe) is exothermic, because of the strong Pd– $\text{CH}(\text{CN})_2$  bond. The CN group stabilizes the  $sp^3$  orbital of alkyl group, which leads to a strengthening of the Pd–alkyl bond. This is easily interpreted in terms of simple perturbation theory.

**Acknowledgment.** This work was supported in part by a Grant-in-Aid for Scientific Research on Priority Areas (No. 09239105) from the Ministry of Education, Science, Sports, and Culture of Japan. B.B. thanks the Ministry of Education, Science, Sports, and Culture of Japan for a scholarship. Computations were carried out with an IBM SP2 machine of the Institute for Molecular Science (Okazaki, Japan) and an IBM RS6000/3CT workstation in our laboratory.

**Supporting Information Available:** Figures showing several possible geometries of the precursor complexes (2 pages). Ordering information is given on any current masthead page.

OM970705I